Desalination and Water Treatment
www.deswater.com

doi: 10.5004/dwt.2019.24421

163 (2019) 281–285
September

Thiourea-assisted sol-gel preparation of ZnO with enhanced photocatalytic performance originated from promoted separation rate of photo-induced carriers

Xinlu Liu, Tao Wang, Junbo Zhong*, Shengtian Huang*, Jianzhang Li

Key Laboratory of Green Catalysis of Higher Education Institutes of Sichuan, College of Chemistry and Environmental Engineering, Sichuan University of Science and Engineering, Zigong, 643000, China, emails: junbozhong@163.com (J. Zhong), sth499@163.com (S. Huang), 34674746@qq.com (X. Liu), 3wangtao3@163.com (T. Wang), lyl63@sina.com (J. Li)

Received 2 January 2019; Accepted 14 May 2019

ABSTRACT

In this work, to further promote the photocatalytic activity of ZnO, T-ZnO with enhanced simulated sunlight-driven photocatalytic activity was prepared by a sol-gel method with the aid of thiourea. The samples were characterized by Brunauer–Emmett–Teller, X-ray diffraction, UV-Vis diffuse reflectance, surface photovoltage spectroscopy and scanning electron microscopy. The level of $^{\bullet}O_2^-$ formed in different photocatalytic systems was compared using nitroblue tetrazolium method. The catalytic properties of the photocatalysts toward elimination of rhodamine B were evaluated under simulated sunlight irradiation. The observations reveal that adding thiourea into the synthetic system of ZnO boosts the photo-induced charge separation rate of ZnO, resulting in enhanced photocatalytic performance. The photocatalytic reaction results exhibit that the photocatalytic activity of T-ZnO is more than twice of that of the reference ZnO (R-ZnO).

Keywords: Semiconductors; Crystal growth; ZnO; Surfaces; Thiourea

1. Introduction

As *n*-type II-VI metal oxide semiconductor, ZnO has drawn considerable interests owing to its exceptional advantages, such as low cost, easy preparation, high electron-mobility and facile electron shuttling property during photocatalytic reactions [1,2]. These entire outstanding properties make ZnO outperform other photocatalysts [3]. However, high recombination rate of photoinduced carriers (e^-–h^+) results in relatively low photocatalytic performances [4,5]. Therefore, it is crucial to ameliorate the photocatalytic efficiency of ZnO by promoting the separation of photo-generated carriers. To achieve this goal, massive strategies have been executed to regulate the photocatalytic activity of ZnO by facilitating the separation of photogenerated carriers [1,6–9].

Photocatalysis takes place on the surface of a semiconductor; therefore the surface properties will definitely affect the adsorption of pollutants on the surface of the photocatalyst and the separation behaviors of the photo-generated carriers [10–12], evidently in turn influencing the photocatalytic properties. From above analysis, it is apparent that the photocatalytic performance of ZnO can be modulated by adjusting the surface properties of ZnO to facilitate the separation of photoinduced carriers.

Our previous results display that the photocatalytic performance of ZnO can be remarkably boosted by a urea-assisted Sol-gel routine [13]. As analogue of urea, it is anticipated that thiourea also can promote the photocatalytic performance of ZnO. Herein, we report a solid and facile method to ameliorate the photocatalytic performance of ZnO with the assistance of thiourea. The results demonstrate that

---

* Corresponding authors.

ZnO prepared with the assistance of thiourea holds higher photocatalytic activity than the reference ZnO.

2. Experimental section

2.1. Preparation of ZnO

ZnO samples were prepared by a typical Sol-gel method as given in the study by Shirdel and Behnajady [14]. Typically, 2.19 g zinc acetate dihydrate was dissolved in 100 mL ethanol at 333 K under vigorous stirring for 30 min, then 20 mL thiourea-ethanol solution was added into the above solution (the molar ratio of N from thiourea/Zn was 0.5%). The mixed solution was marked as solution A. 2.51 g oxalic acid was dissolved in 40 mL ethanol at 333 K and designed as solution B. Solution B was added dropwise into the solution A, and then continuously stirred to form a gel. The dried gel was calcined at 673 K for 2 h; the sample was designed as T-ZnO. For comparison, the reference ZnO was prepared as the above recipe absent of thiourea and named as R-ZnO.

2.2. Characterization of ZnO samples

Brunauer–Emmett–Teller (BET) specific surface area measurements were carried out on a SSA-4200 automatic surface analyzer. X-ray diffraction (XRD) patterns were collected on a DX-2600 X-ray diffractometer using Cu Kα radiation. Scanning electron microscopy (SEM) and energy dispersive spectrometer (EDS) were performed by using a JSM-7500F. Optical properties were analyzed on a TU-1907 UV-vis spectrophotometer. Surface photovoltage spectroscopy (SPS) was employed to investigate the separation behaviors of photo-generated charge pairs on a homemade apparatus MODEL SR540 surface photovoltage spectrometer from 300 to 600 nm. SPS was measured on a solid junction photovoltaic cell (ITO/sample/ITO) using light source-monochromator-lock-in detection technique, the principle of SPS measurement was described in [15,16]. The level of $^{\bullet}O_2^-$ radicals was investigated using nitroblue tetrazolium (NBT) method as described in [17].

2.3. Photocatalysis

The photocatalytic abilities of two photocatalysts (T-ZnO and R-ZnO) toward decomposition of rhodamine B (RhB) aqueous solution (50 mL, pH = 7.0) were evaluated under simulated sunlight illumination. The detailed procedures were stated in the study by Liu et al. [18]. The irradiation source was a 500 W Xe lamp. The dosage of photocatalyst was 1 g/L, and the volume of RhB solution was 50 mL. The photocatalysis was performed at room temperature. At regular timespans, the samples were removed and centrifuged to separate the photocatalyst and the absorbance of the supernatant was measured at 554 nm. The decolorization (D) efficiency was determined as follows:

$$D = \frac{A_0 - A}{A_0} \times 100\%$$

where A_0 and A are the absorbance of RhB before and after photocatalytic reaction, respectively.

3. Results and discussion

3.1. Characterization results of the samples

The specific surface area for R-ZnO and T-ZnO is 24.4 and 26.3 m^2/g, respectively. In view of the measurement error (±5 m^2/g), two samples have no distinctly difference in specific surface area. Similar results were observed when urea was employed to prepare ZnO [13], which indicates that thiourea cannot affect the specific surface area of ZnO due to the removal of thiourea during baking process.

The XRD patterns of two samples are exhibited in Fig. 1. According to the reported data (JCPDS No. 79-0206), it is apparent that all the strong peaks can be attributed to the pure hexagonal phase of wurtzite-type ZnO. No peaks of impurities were detected, implying high purity of the samples. Moreover, the diffraction peak intensities of two samples have no distinct difference, suggesting that two samples have similar crystal size, which accords well with the results of S_{BET}.

The microstructures of the two samples are exhibited in Fig. 2. It is evident that both two samples display lump-like morphologies, indicating that the shape of the sample cannot be affected by thiourea. The shape of ZnO depends on the essence of the preparation processes and precursors. During the calcination process of ZnO, thiourea was completely oxidized. Consequently, the shape of ZnO cannot be altered by thiourea. Fig. 2c shows the EDS result of T-ZnO. Only C, O and Zn elements were observed and no S element was detected; therefore the influence of the residual S is ignorable.

As demonstrated in Fig. 3 (inset), two samples exhibit similar optical absorbance, which suggests that no S was doped into the lattice of ZnO or the effect of S on the band-gap can be totally ignored. Although thiourea cannot affect the specific surface area, the crystal structure, morphology and band gap, the presence of thiourea in the synthetic system promotes the separation of photo-induced carriers, as displayed in Fig. 3. It is obvious that the T-ZnO holds stronger SPS response than R-ZnO. The SPS peak value of T-ZnO is more than twice of that of R-ZnO, which suggests that adding thiourea into the synthetic system alters

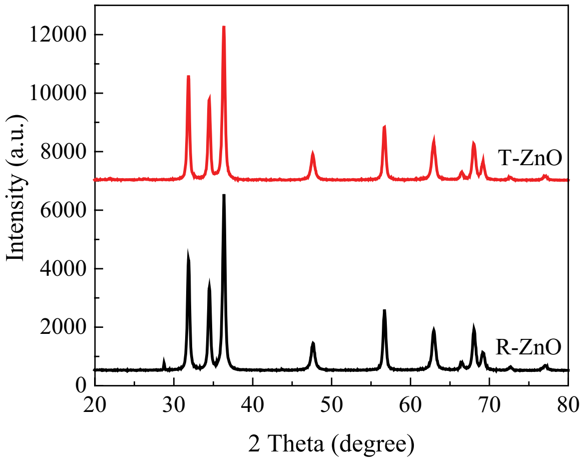

Fig. 1. Crystal structures of the samples as prepared.

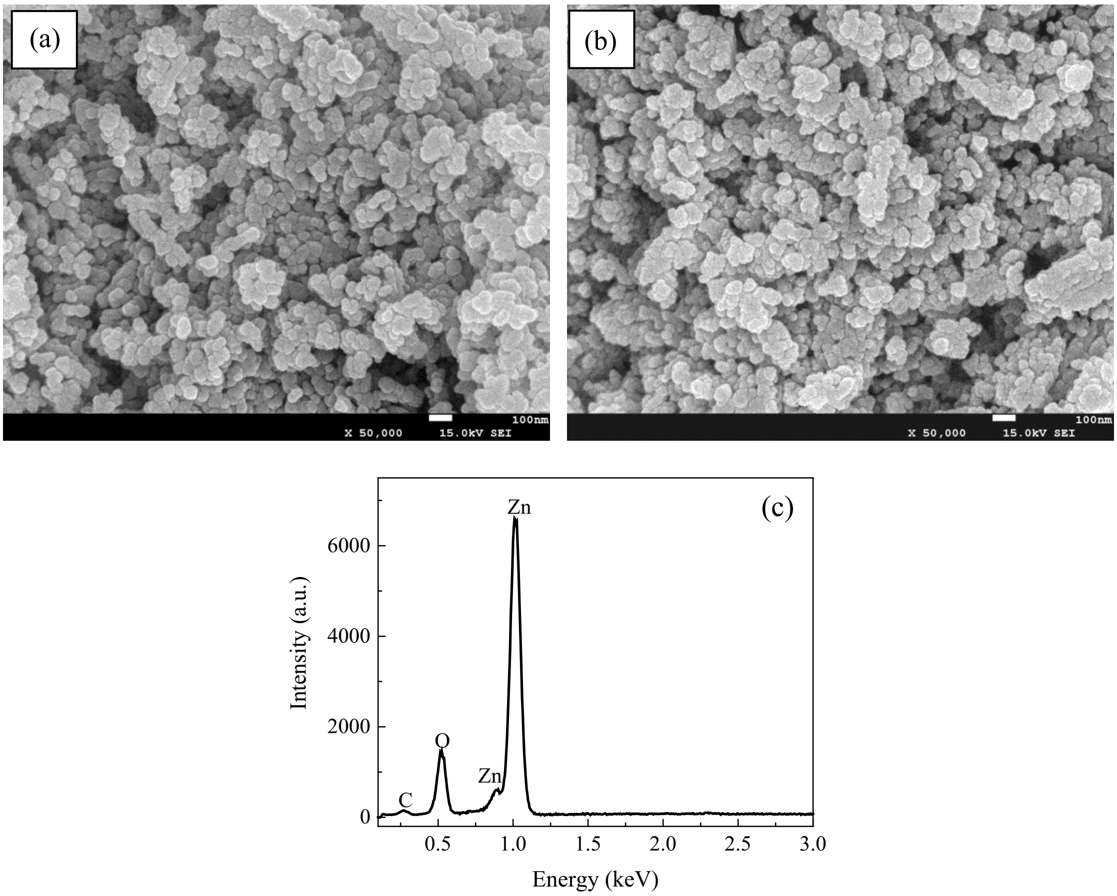

Fig. 2. SEM images of (a) R-ZnO, (b) T-ZnO, and (c) EDS pattern of T-ZnO.

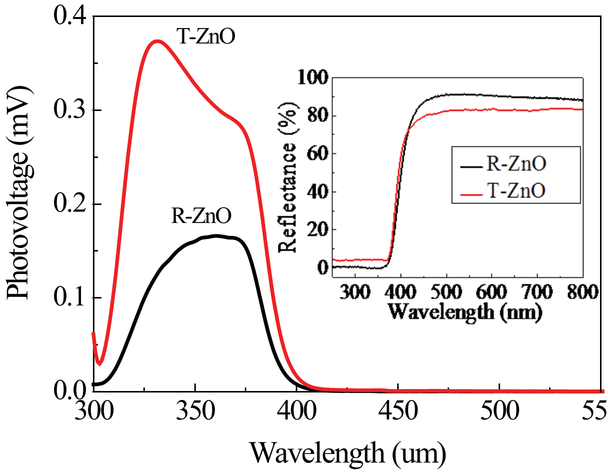

Fig. 3. SPS responses of the samples, the inset is the UV-Vis DRS.

the surface states of ZnO, promoting the separation of photogenerated carriers. Similar results were observed when urea was employed to prepare ZnO [13]. Generally, strong SPS signal implies high separation rate of photogenerated carriers [19], therefore, the separation rate of photogenerated carriers of T-ZnO is more than twice than that of R-ZnO. It is well recognized that separation rate of photogenerated carriers plays leading role in affecting the photocatalytic performances [20]. It is naturally anticipated that T-ZnO would display higher photocatalytic ability than R-ZnO, which can be firmly supported by the results of photocatalysis (see Fig. 6).

To further reveal the effects of thiourea in the synthetic process on the formation of active free radicals, trapping and NBT experiments were performed. As shown in Fig. 4, isopropanol (IPA, for $^{\bullet}OH$), ammonium oxalate (AO, for h^+) and benzoquinone (BQ, for $^{\bullet}O_2^-$) execute different effects on the elimination of RhB. It is evident that BQ remarkably restrains the decay of RhB. The decay efficiency of RhB is the lowest after adding BQ into the photocatalytic reaction system, the result firmly indicates that $^{\bullet}O_2^-$ is the primary active free radicals, which accords well with our previous results [21].

NBT is a water-soluble substance with absorption peak at 259 nm, which can combine with four superoxide anions to form a purple water-insoluble substance [13]. Therefore, NBT was chosen to investigate the relative level of $^{\bullet}O_2^-$ generated in different photocatalytic systems. To further investigate the effects of thiourea in the synthetic process on the level of $^{\bullet}O_2^-$, NBT experiments were carried out. As demonstrated in Fig. 5, the presence of thiourea in the synthetic system of ZnO indeed affects the level of

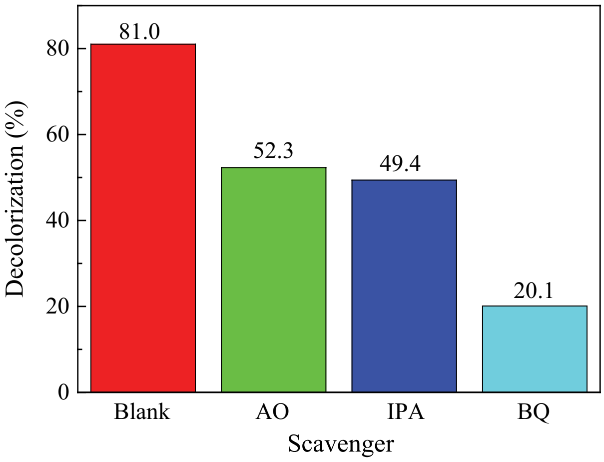

Fig. 4. Effects of scavengers on RhB degradation over T-ZnO (illumination time = 20 min, scavenger dosage = 0.2 mmol/L).

$^{\bullet}O_2^-$ generated in the photocatalytic system. According to the exclusive reaction between $^{\bullet}O_2^-$ and NBT, high level of $^{\bullet}O_2^-$ in the photocatalytic system will result in low absorbance of NBT [17]. The results indicate that the relatively higher separation rate of photo-induced carries results in high level of $^{\bullet}O_2^-$ prepared. In general, high separation efficiency of photo-generated charge and high level of $^{\bullet}O_2^-$ will expedite the degradation of RhB, manifesting high photocatalytic performances. The results agree well with the result of photocatalytic activities and SPS.

3.2. Photocatalytic properties

The adsorption of RhB on two photocatalysts and the photolysis of RhB after 20 min are less than 4% and can be neglected. Photocatalytic abilities of two samples toward decay of RhB were evaluated. As exhibited in Fig. 6, the photolysis of RhB under the simulated sunlight irradiation without photocatalyst is less than 6%. Therefore, RhB will not be degraded without photocatalyst under the irradiation of simulated sunlight for 20 min. As expected, T-ZnO displays higher photocatalytic activity than R-ZnO. Additionally, the elimination of RhB over two photocatalysts follows a first-order kinetics. The decay rate constants of RhB over two photocatalysts are 0.039 and 0.081 min^{-1}, respectively. Obviously, the decay rate constant of RhB over T-ZnO is more than twice of that over R-ZnO. In view of low loading and cost of thiourea, thiourea-assisted sol-gel fabrication of ZnO is an effective and solid strategy to regulate the photocatalytic ability of ZnO by expediting the separation of photoinduced carriers. It is quite promising that this method can be employed to prepare other photocatalysts with exceptional photocatalytic abilities.

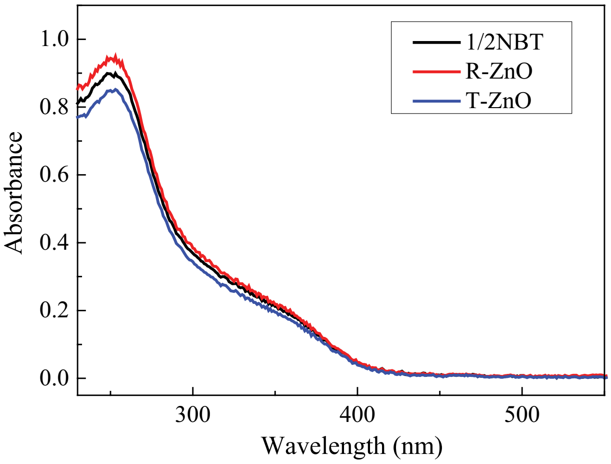

Fig. 5. Absorbance of NBT in different photocatalytic systems (illumination time = 20 min, NBT dosage = 0.05 mmol/L).

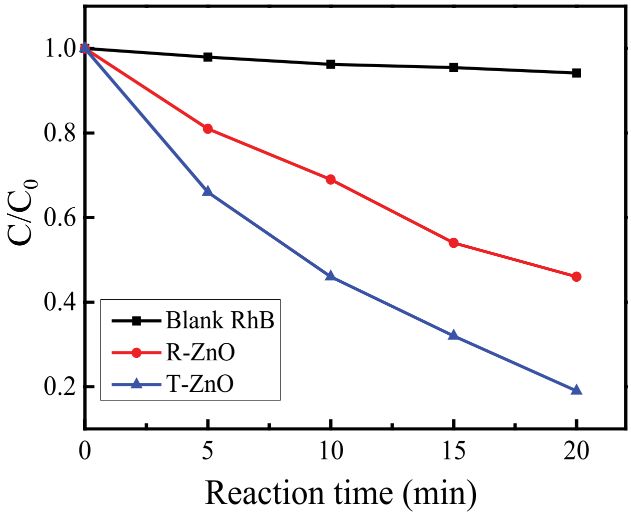

Fig. 6. Decay of RhB over two photocatalyst.

4. Conclusions

In summary, wurtzite-type ZnO photocatalyst with boosted sunlight-driven photocatalytic activity was obtained by a typical sol-gel approach with the assistance of thiourea. The results reveal that the photocatalytic performance of ZnO prepared with the assistance of thiourea is more than twice of that of the reference ZnO. The enhanced photocatalytic performance of ZnO toward elimination of RhB tightly relates to the improved photo-induced carriers separation rate. Thiourea-assisted fabrication of ZnO is an effective and solid strategy to promote the photocatalytic ability of ZnO.

Acknowledgements

This project was financially supported by the program of Science and Technology Department of Sichuan province (No.2017096), Students Innovation Project of Sichuan Province (No. 201710622065) and the Project of Zigong city (No. 2016HG06).

References

[1] K.M. Lee, C.W. Lai, K.S. Ngai, J.C. Juan, Recent developments of zinc oxide based photocatalyst in water treatment technology: a review, Water Res., 88 (2016) 428–448.

[2] J.Y. Xiong, Y.X. Gan, J.X. Zhu, W. Li, C. Gao, Y. Wei, G. Cheng, Z. Li, S.X. Dou, Insights into the structure-induced catalysis dependence of simply engineered one-dimensional zinc oxide nanocrystals towards photocatalytic water purification, Inorg. Chem. Front., 4 (2017) 2075–2087.

[3] S. Jayswal, R.S. Moirangthem, Construction of a solar spectrum active SnS/ZnO p–n heterojunction as a highly efficient photocatalyst: the effect of the sensitization process on its performance, New J. Chem., 42 (2018) 13689–13701.

[4] B. Xue, Y.Q. Zou, Uniform distribution of ZnO nanoparticles on the surface of graphene and its enhanced photocatalytic performance, Appl. Surf. Sci., 440 (2018) 1123–1129.

[5] G.M. Neelgund, A. Oki, Photothermal effect: an important aspect for the enhancement of photocatalytic activity under illumination by NIR radiation, Mater. Chem. Front., 2 (2018) 64–75.

[6] A.N. Kadam, D.P. Bhopate, V.V. Kondalkar, S.M. Majhi, C.D. Bathula, A.-V. Tran, S.-W. Lee, Facile synthesis of Ag-ZnO core–shell nanostructures with enhanced photocatalytic activity, J. Ind. Eng. Chem., 61 (2018) 78–86.

[7] F.X. Wang, L. Liang, L. Shi, M.S. Liu, J.M. Sun, CO_2-assisted synthesis of mesoporous carbon/C-doped ZnO composites for enhanced photocatalytic performance under visible light, Dalton Trans., 43 (2014) 16441–16449.

[8] Y.-H. Chiu, K.-D. Chang, Y.-J. Hsu, Plasmon-mediated charge dynamics and photoactivity enhancement for Au-decorated ZnO nanocrystals, J. Mater. Chem. A., 6 (2018) 4286–4296.

[9] D.Q. Xu, Y.W. Bai, Z.R. Li, Y. Guo, L. Bai, Enhanced photodegradation ability of solvothermally synthesized metallic copper coated ZnO microrods, Colloids Surf., A, 548 (2018) 19–26.

[10] X.W. Zheng, H.H. Liu, J.B. Zhong, S.T. Huang, J.Z. Li, D.M. Ma, Remarkably enhanced sunlight-driven photocatalytic performance of TiO_2 by facilely modulating the surface property, Mater. Sci. Semicond. Process., 74 (2018) 109–115.

[11] D.M. Ma, J.B. Zhong, J.Z. Li, L. Wang, R. Peng, Enhanced photocatalytic activity of BiOCl by C_{70} modification and mechanism insight, Appl. Surf. Sci., 443 (2018) 497–505.

[12] Y.J. Si, H.H. Liu, N.T. Li, J.B. Zhong, J.Z. Li, D.M. Ma, SDBS-assisted hydrothermal treatment of TiO_2 with improved photocatalytic activity, Mater. Lett., 212 (2018) 147–150.

[13] X.L. Liu, J.F. Chen, J.Z. Li, J.B. Zhong, T. Wang, Enhanced sunlight-driven photocatalytic performance of ZnO prepared with the assistance of urea, Desal. Wat. Treat, 132 (2018) 226–234.

[14] B. Shirdel, M.A. Behnajady, Sol-gel synthesis of Ba-doped ZnO nanoparticles with enhanced photocatalytic activity in degrading Rhodamine B under UV-A irradiation, Optik, 147 (2017) 143–150.

[15] P. Wang, D.J. Wang, H.Y. Li, T.F. Xie, H.Z. Wang, Z.L. Du, A facile solution-phase synthesis of high quality water-solution anatase TiO_2 nanocrystals, J. Colloid Interface Sci., 314 (2007) 337–340.

[16] Y.H. Lin, D.J. Wang, Q.D. Zhao, M. Yang, Q.L. Zhang, A study of quantum confinement properties of photogenerated charges in ZnO nanoparticles by surface photovoltage spectroscopy, J. Phys. Chem. B, 108 (2004) 3203–3206.

[17] L.Q. Ye, J.Y. Liu, Z. Jiang, T.Y. Peng, L. Zan, Facets coupling of BiOBr-g-C_3N_4 composite photocatalyst for enhanced visible-light-driven photocatalytic activity, Appl. Catal., B, 142–143 (2013) 1–7.

[18] X.L. Liu, J.B. Zhong, J.Z. Li, S.T. Huang, W. Song, PEG-assisted hydrothermal synthesis of BiOCl with enhanced photocatalytic performance, Appl. Phys. A, 119 (2015) 1203–1208.

[19] D.M. Ma, J.B. Zhong, R.F. Peng, J.Z. Li, R. Duan, Effective photoinduced charge separation and photocatalytic activity of hierarchical microsphere-like C_{60}/BiOCl, Appl. Surf. Sci., 465 (2019) 249–258.

[20] X.W. Zheng, Q. Yang, S.T. Huang, J.B. Zhong, J.Z. Li, R.H. Yang, Y.Y. Zhang, Enhanced separation efficiency of photo-induced charge pairs and sunlight-driven photocatalytic performance of TiO_2 prepared with the assistance of NH_4Cl, J. Sol-Gel Sci. Technol., 83 (2017) 174–180.

[21] Z. Xiang, J.B. Zhong, S.T. Huang, J.Z. Li, J.F. Chen, T. Wang, M.J. Li, P. Wang, Efficient charge separation of Ag_2CO_3/ZnO composites prepared by a facile precipitation approach and its dependence on loading content of Ag_2CO_3, Mater. Sci. Semicond. Process., 52 (2016) 62–67.